LAMINAR FLOW IN CONCENTRIC ANNULUS WITH A MOVING CORE

Mohamed F. Khalil, Sadek Z. Kassab, Ihab G. Adam, and Mohamed Samaha

Mechanical Engineering Department,
Faculty of Engineering, Alexandria University, Alexandria 21544, Egypt
E-mails: mfaridkhalil@yahoo.com , szkassab@yahoo.com
ihabadam@yahoo.com , moh_samaha@yahoo.com

ABSTRACT

An analytical solution and a numerical analysis are presented to study the flow behavior in concentric annulus with moving core in pipe for laminar flow condition. The analytical analysis is presented as exact solution for steady, fully developed and one dimensional flow. The numerical model is presented to study two-dimensional, steady, developing and fully developed flows. The numerical model established a staggered grid for axial and radial velocities (V_z and V_r) and using the pressure correction technique. The analyses were used to predict not only the fully developed velocity profile for negative, zero, and adverse pressure gradient but also the developing velocity profiles until the flow becomes fully developed. The developing length (entrance length), the boundary layer thickness and the pressure distribution along the moving core at different Reynolds numbers are also obtained by the presented model. The drag coefficient relative to both the moving core wall and the pipe wall can be calculated at different Reynolds numbers and diameter ratios. The results of the laminar model were shown to be in good agreement with the analytical (exact) solution for the fully developed flow. This also gives confidence to the obtained results for the developing flow through the entrance length using the numerical model.

Keywords: Developing and Fully developed, Laminar flow, Concentric annulus, Pipe flow, Moving Core, Numerical model, Staggered grid, Pressure correction technique.

INTRODUCTION

The laminar flow in annulus was analyzed by different researchers to predict the flow properties such as the pressure drop, velocity profiles…etc. These analyses were used to predict capsule flow performance in hydraulic capsule pipeline systems. Govier and Aziz (1972) presented an overview, general theoretical and experimental analysis for concentric and eccentric, Laminar and Turbulent capsule flow in a pipeline. They studied both cylindrical and spherical shapes of capsule. Garg (1977) presented an improved theoretical analysis for a rigid, smooth, cylindrical capsule moving parallel

to the horizontal pipe wall by taking into account the friction between the capsule and the pipe surfaces. In addition, Garg (1977) studied the non-uniform clearance over the capsule length to investigate its effect on the capsule pipeline operation and design. Theoretical analysis for laminar eccentric capsule flow is presented by Garner and Raithby (1978) to estimate the capsule velocity, and the velocity profiles in the annulus.

The capsule velocity and the pressure drop across the capsule in both hydraulic and pneumatic pipelines are analyzed for laminar flow by Tomita and Fujiwara (1992). Fujiwara et al. (1994) used the method of characteristics to study the hydraulic capsule transport parameters such as the pressure drop, capsule velocity, capsule specific gravity, and the type of flow (i.e. laminar or turbulent). Laminar-Turbulent velocity profile transition for flows in concentric Annuli, Parallel Plates and Pipes were modeled numerically by Ogawa et al. (1980) to predict the velocity profile and the pressure gradient. A theoretical analysis by using the method of characteristics for capsule Pipeline flow is performed by Tomita et al. (1981) to estimate the capsule and the mean velocities, to investigate the effect of the exhaust valve on the capsule motion, and to plot the time history of the pressure along the pipeline compared with the experimental data. Tachibana (1983) study the balance and the start up of cylindrical capsule in rising flow of inclined pipeline by presenting a theoretical model depending on the method of characteristics and the experimental data. The wake of capsule and the effect of interaction between two capsules on the drag are studied experimentally by Tsuji et al. (1984).

An Overview on freight pipelines: current status and anticipated future use was done by Liu (1998) in that the basic concept, specifications, history, classification, system components, system operation, economics, expected and obstacles to future use, method of capsules injection, advantages, disadvantages, and applications are explained for several types of the freight pipelines (such as pneumatic pipelines, slurry pipelines, pneumatic capsule pipelines, and hydraulic capsule pipelines). Liu in his book Pipeline Engineering (2003) gave a complete chapter on the capsule pipeline technology, history, systems descriptions and types, flow analysis, design examples, capsule pumping, capsule injection and ejection, and coal log pipeline technology as an application on Hydraulic Capsule Pipeline, HCP.

As a first step towards studying the capsule pipeline (more details are given by Samaha (2007)), the present study concerned with the flow through the annulus between concentric moving core and Pipe. The region under consideration is the developing region starting from the uniform velocity distribution at the annulus inlet until the velocity profile reaches the fully developed shape where there is no change with respect to the distance along the core length. The fully developed case is solved using analytical solution. Meanwhile the solution within the developing region is obtained using numerical solution where there is no analytical solution. In addition, the fully developed case can be obtained using the numerical solution. This gives a chance for comparing the exact analytical solution with the obtained numerical one for the case of fully developed flow. This comparison sheds some light on the accuracy and

credibility of the results of the numerical solution within the developing region where there is no analytical solution available.

PROBLEM DESCRIPTION

The problem as shown in Figure 1 is described as a single long moving core in concentric position in a pipe that can be solved for different core to pipe diameter ratios, different core velocity, and at different annular Reynolds number Re_p relative to pipe wall. The fluid around the core is water. The flow enters at the core tail as uniform flow.

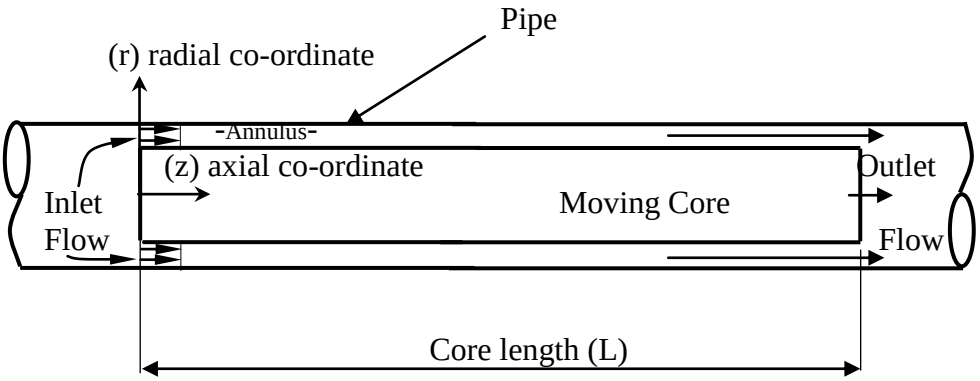

Figure 1 Schematic illustration for long concentric moving core in pipe

GENERAL CONSIDERATIONS

The present study is primarily concerned with modeling the two dimensional Axi-symmetric laminar flow in annulus between concentric moving core and Pipe. The flow in the entrance region (Developing region) in the annulus at the core tail is considered two-dimensional flow where the velocity profile is changed from uniform flow until it reaches the fully developed velocity profile where the velocity profile become unchanged with respect to the distance along the core length.

The numerical solution is performed by solving the two momentum equations (in [z] and [r] directions) to find the two components of velocity in the two direction of the flow (V_z and V_r) and solving the continuity equation to check if the pressure gradient should be corrected or not to satisfy this continuity equation so that this rule is called the Pressure Correction Technique.

The following assumptions are taken into account to solve the present problem.

1. Incompressible Laminar and steady flow.
2. Newtonian fluid.
3. The temperature and the fluid viscosity are assumed constant.

4. Axi-symmetric, flow (in z- and in r-directions only). Assume the center line of the moving core is coincided with the center line of the pipe.
5. Horizontal flow with no body forces.
6. The pressure gradient in (z)-axial direction is considered only. The pressure gradient in (r)-radial direction is neglected where the pressure is approximately the same in the same section.
7. The term ($\partial V / \partial t$) is used for iterations.

GOVERNING EQUATIONS

The governing equations to solve the two dimensional axi-symmetric laminar flow are the momentum equation in the flow direction (in z-direction) and in the radial direction (in r-direction). There is also one unknown term in the momentum equations that is the pressure gradient. This term can be estimated by assuming it then try to correct it until the continuity equation is satisfied (Pressure correction technique).

Momentum equation in r-direction

$$\rho\left(\frac{\partial V_r}{\partial t}+V_r\frac{\partial V_r}{\partial r}+V_z\frac{\partial V_r}{\partial z}\right)=\left[\frac{1}{r}\frac{\partial}{\partial r}r(\mu)\frac{\partial V_r}{\partial r}\right]-(\mu)\frac{V_r}{r^2}+(\mu)\frac{\partial^2 V_r}{\partial z^2} \tag{1}$$

Momentum equation in z-direction

$$\rho\left(\frac{\partial V_z}{\partial t}+V_r\frac{\partial V_z}{\partial r}+V_z\frac{\partial V_z}{\partial z}\right)=-\frac{\partial P}{\partial z}+\left[\frac{1}{r}\frac{\partial}{\partial r}r(\mu)\frac{\partial V_z}{\partial r}\right]+(\mu)\frac{\partial^2 V_z}{\partial z^2} \tag{2}$$

But these equations are in the non-conservative forms so they must be converted to the conservative forms to give a facility of deriving the finite difference formulas by solving these momentum equations with the continuity equation:

$$\left(\frac{V_r}{r}+\frac{\partial V_r}{\partial r}+\frac{\partial V_z}{\partial z}\right)=0 \tag{3}$$

So the momentum equations can be rewritten as:

In r-direction

$$\rho\left(\frac{\partial V_r}{\partial t}+\frac{\partial V_r^2}{\partial r}+\frac{\partial V_z V_r}{\partial z}+\frac{V_r^2}{r}\right)=\left[\frac{1}{r}\frac{\partial}{\partial r}r(\mu)\frac{\partial V_r}{\partial r}\right]-(\mu)\frac{V_r}{r^2}+(\mu)\frac{\partial^2 V_r}{\partial z^2} \tag{4}$$

Rearranging the momentum equation terms as:

$$\rho\left(\frac{\partial V_r}{\partial t}+\frac{\partial V_z V_r}{\partial z}+2V_r\ \frac{\partial V_r}{\partial r}+\frac{V_r^2}{r}\right)=\left[(\mu)(\frac{\partial^2 V_r}{\partial r^2}+\frac{1}{r}\frac{\partial V_r}{\partial r})\right]-(\mu)\frac{V_r}{r^2}+(\mu)\frac{\partial^2 V_r}{\partial z^2} \quad (5)$$

Also in z-direction:

$$\rho\left(\frac{\partial V_z}{\partial t}+\frac{\partial V_z V_r}{\partial r}+\frac{\partial V_z^2}{\partial z}+\frac{V_z V_r}{r}\right)=-\frac{\partial P}{\partial z}+\left[\frac{1}{r}\frac{\partial}{\partial r}r(\mu)\frac{\partial V_z}{\partial r}\right]+(\mu)\frac{\partial^2 V_z}{\partial z^2} \quad (6)$$

Rearranging the momentum equation terms as:

$$\rho\left(\frac{\partial V_z}{\partial t}+\frac{\partial V_z V_r}{\partial r}+2V_z\frac{\partial V_z}{\partial z}+\frac{V_z V_r}{r}\right)=-\frac{\partial P}{\partial z}+\left[(\mu)(\frac{\partial^2 V_z}{\partial r^2}+\frac{1}{r}\frac{\partial V_z}{\partial r})\right]+(\mu)\frac{\partial^2 V_z}{\partial z^2} \quad (7)$$

and

$$\tau_w=\mu\left[\frac{\partial V_z}{\partial r}+\frac{\partial V_r}{\partial z}\right] \quad (8)$$

By referring to Figure 1, the boundary conditions are shown as:

1- The Velocity profile at the inlet to the annulus is uniform $V_z = V_a$ and the radial velocity $V_r = 0$.
2- The axial and the radial velocities at the pipe wall equal to zero (no slip condition).
3- The axial velocity equal to the moving core velocity and the radial velocity equal to zero at the moving core wall (no slip condition).
4- The outlet flow is defined by extrapolating the flow properties (V_z, V_r and dP/dz).

STAGGERED GRID AND FINITE DIFFERENCE EQUATIONS

A staggered grid is used as shown in Figure 2. The pressure gradient is calculated at the solid points i.e. (i, j), (i+1, j), (i, j+1) ...etc. The axial velocity V_z is calculated at the opened points ($i+\frac{1}{2}$, j), ($i+\frac{3}{2}$, j), ($i+\frac{1}{2}$, j+1) ...etc. The radial velocity V_r is calculated at the opened points ($i, j+\frac{1}{2}$), ($i, j+\frac{3}{2}$), (i+1, $j+\frac{1}{2}$) ...etc.

Note that, the need for a staggered grid is to satisfy velocity distribution to be basically sense to real physical flow field (Anderson 1995).

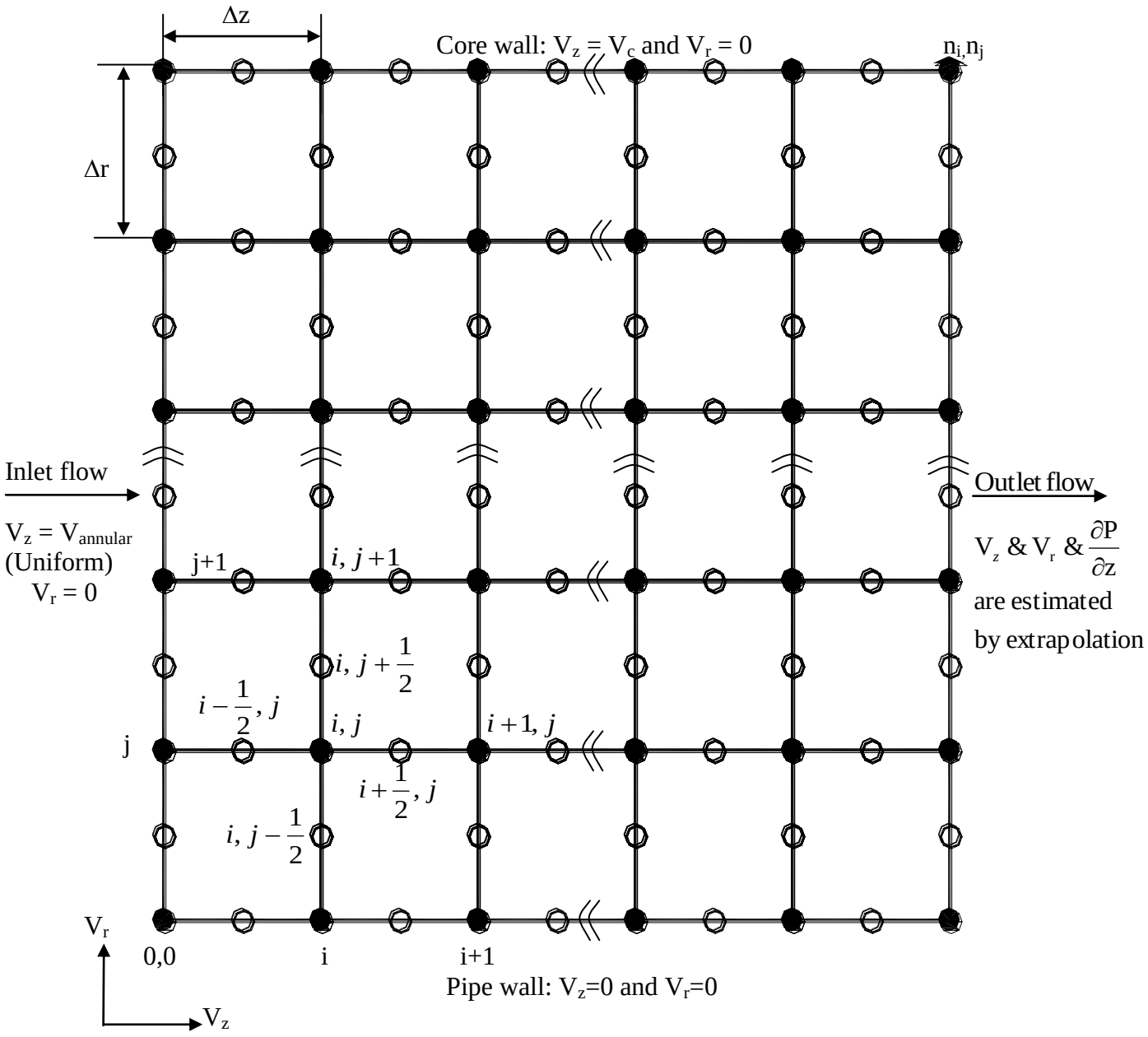

Figure 2 Staggered grid points

Momentum equation in z-direction

Referring to Anderson (1995), one uses Implicit Forward differencing in time, backward differencing in z-direction (Upwinding) and central differencing in r-direction. The forward differencing in time must be considered because the new time step information should be calculated from the previous step but the vise verse is physically insensitive. The backward differencing in z-direction (first upwind scheme) is considered because the flow velocity profiles are solved line by line i.e. the front line information is calculated from the back line information where the inlet

information is known. The central differencing in r-direction is considered because the information about both core and pipe boundary conditions are known.

Note that for the diffusion term $\frac{\partial^2 V_z}{\partial z^2}$ must be central differencing instead of backward differencing where the backward differencing makes the scheme solution unstable (Anderson 1995). The finite divided difference equation at general point (i+$\frac{1}{2}$, j) can be, in accordance, written as:

$$\rho\left(\frac{(V_z)^{n+1}_{i+\frac{1}{2},j}-(V_z)^{n}_{i+\frac{1}{2},j}}{\Delta t}+2(V_z)^{n}_{i+\frac{1}{2},j}\frac{(V_z)^{n+1}_{i+\frac{1}{2},j}-(V_z)^{n+1}_{i-\frac{1}{2},j}}{\Delta z}+\frac{\left(V_z{}^{n+1}\overline{V_r}^{\,n}\right)_{i+\frac{1}{2},j+1}-\left(V_z{}^{n+1}\overline{V_r}^{\,n}\right)_{i+\frac{1}{2},j-1}}{2\Delta r}\right)$$

$$+\rho\frac{\left(V_z{}^{n+1}\overline{V_r}^{\,n}\right)_{i+\frac{1}{2},j}}{r_j}=-\left(\frac{\partial P}{\partial z}\right)^{n}_{i,j}+\left[(\mu)\left(\frac{(V_z)^{n+1}_{i+\frac{1}{2},j+1}-2(V_z)^{n+1}_{i+\frac{1}{2},j}+(V_z)^{n+1}_{i+\frac{1}{2},j-1}}{(\Delta r)^2}+\frac{1}{r_j}\frac{(V_z)^{n+1}_{i+\frac{1}{2},j+1}-(V_z)^{n+1}_{i+\frac{1}{2},j-1}}{2\Delta r}\right)\right]$$

$$+\left[(\mu)\frac{(V_z)^{n+1}_{i+\frac{3}{2},j}-2(V_z)^{n+1}_{i+\frac{1}{2},j}+(V_z)^{n+1}_{i-\frac{1}{2},j}}{(\Delta z)^2}\right] \tag{9}$$

Rearrange Equation (9):

$$\left[1+2(V_z)^{n}_{i+\frac{1}{2},j}\frac{\Delta t}{\Delta z}+\Delta t\frac{\left(\overline{V_r}^{\,n}\right)_{i+\frac{1}{2},j}}{r_j}-\frac{\mu\Delta t}{\rho}\left(\frac{-2}{\Delta z^2}-\frac{2}{\Delta r^2}\right)\right](V_z)^{n+1}_{i+\frac{1}{2},j}$$

$$+\left[\Delta t\frac{\left(\overline{V_r}^{\,n}\right)_{i+\frac{1}{2},j+1}}{2\Delta r}-\frac{\mu\Delta t}{\rho}\left(\frac{1}{\Delta r^2}+\frac{1}{r_j}\frac{1}{2\Delta r}\right)\right](V_z)^{n+1}_{i+\frac{1}{2},j+1}$$

$$+\left[-\Delta t\frac{\left(\overline{V_r}^{\,n}\right)_{i+\frac{1}{2},j-1}}{2\Delta r}-\frac{\mu\Delta t}{\rho}\left(\frac{1}{\Delta r^2}-\frac{1}{r_j}\frac{1}{2\Delta r}\right)\right](V_z)^{n+1}_{i+\frac{1}{2},j-1} \tag{10}$$

$$=(V_z)^{n}_{i+\frac{1}{2},j}+2(V_z)^{n}_{i+\frac{1}{2},j}\frac{(V_z)^{n+1}_{i-\frac{1}{2},j}}{\Delta z}\Delta t-\frac{\Delta t}{\rho}\left(\frac{\partial P}{\partial z}\right)^{n}_{i,j}+\left(\frac{\mu\Delta t}{\rho}\right)\frac{(V_z)^{n+1}_{i+\frac{3}{2},j}+(V_z)^{n+1}_{i-\frac{1}{2},j}}{(\Delta z)^2}$$

Equation (10) can be written in simpler form as follows:

$$b_j \left(V_z\right)^{n+1}_{i+\frac{1}{2},j-1} + d_j \left(V_z\right)^{n+1}_{i+\frac{1}{2},j} + a_j \left(V_z\right)^{n+1}_{i+\frac{1}{2},j+1} = c_j \tag{11}$$

where

$$b_j = \left[1 + 2\left(V_z\right)^{n}_{i+\frac{1}{2},j} \frac{\Delta t}{\Delta z} + \Delta t \frac{\left(\overline{V_r}^{\,n}\right)_{i+\frac{1}{2},j}}{r_j} - \frac{\mu \Delta t}{\rho}\left(\frac{-2}{\Delta z^2} - \frac{2}{\Delta r^2}\right)\right] \tag{12}$$

$$d_j = \left[\Delta t \frac{\left(\overline{V_r}^{\,n}\right)_{i+\frac{1}{2},j+1}}{2\Delta r} - \frac{\mu \Delta t}{\rho}\left(\frac{1}{\Delta r^2} + \frac{1}{r_j}\frac{1}{2\Delta r}\right)\right] \tag{13}$$

$$a_j = \left[-\Delta t \frac{\left(\overline{V_r}^{\,n}\right)_{i+\frac{1}{2},j-1}}{2\Delta r} - \frac{\mu \Delta t}{\rho}\left(\frac{1}{\Delta r^2} - \frac{1}{r_j}\frac{1}{2\Delta r}\right)\right] \tag{14}$$

$$c_j = \left(V_z\right)^{n}_{i+\frac{1}{2},j} + 2\left(V_z\right)^{n}_{i+\frac{1}{2},j} \frac{\left(V_z\right)^{n+1}_{i-\frac{1}{2},j}}{\Delta z}\Delta t - \frac{\Delta t}{\rho}\left(\frac{\partial P}{\partial z}\right)^{n}_{i,j} + \left(\frac{\mu \Delta t}{\rho}\right)\frac{\left(V_z\right)^{n+1}_{i+\frac{3}{2},j} + \left(V_z\right)^{n+1}_{i-\frac{1}{2},j}}{(\Delta z)^2} \tag{15}$$

Equation (11) can be solved by Gauss elimination technique which is programmed in Thomas algorithm. Note that $\overline{V_r}$ is calculated using extrapolation because V_r use different grid points than those of V_z and the next point $(V_z)^{n+1}_{i+\frac{3}{2}}$ is calculated by extrapolation also.

Momentum equation in r-direction

As explained previously, forward differencing in time must be used, backward differencing in z-direction (Upwinding) and central differencing in r-direction. The diffusion term $\frac{\partial^2 V_z}{\partial z^2}$ must be central differencing.

The finite divided difference equation at general point (i, j+$\frac{1}{2}$) can be, in accordance, written as:

$$\rho\left(\frac{(V_r)^{n+1}_{i,j+\frac{1}{2}}-(V_r)^{n}_{i,j+\frac{1}{2}}}{\Delta t}+(V_r)^{n}_{i,j+\frac{1}{2}}\frac{(V_r)^{n+1}_{i,j+\frac{3}{2}}-(V_r)^{n+1}_{i,j-\frac{1}{2}}}{\Delta r}+\frac{(V_r\overline{V_z})^{n+1}_{i,j+\frac{1}{2}}-(V_r\overline{V_z})^{n+1}_{i-1,j+\frac{1}{2}}}{\Delta z}\right)$$

$$\rho\frac{(V_r{}^{n}V_r{}^{n+1})_{i,j+\frac{1}{2}}}{r_{j+\frac{1}{2}}}=\left[(\mu)\left(\frac{(V_r)^{n+1}_{i,j+\frac{3}{2}}-2(V_r)^{n+1}_{i,j+\frac{1}{2}}+(V_r)^{n+1}_{i,j-\frac{1}{2}}}{(\Delta r)^2}+\frac{1}{r_{j+\frac{1}{2}}}\frac{(V_r)^{n+1}_{i,j+\frac{3}{2}}-(V_r)^{n+1}_{i,j-\frac{1}{2}}}{2\Delta r}\right)\right]$$

$$-(\mu)\frac{(V_r)^{n+1}_{i,j+\frac{1}{2}}}{r^2_{j+\frac{1}{2}}}+\left[(\mu)\frac{(V_r)^{n+1}_{i+1,j+\frac{1}{2}}-2(V_r)^{n+1}_{i,j+\frac{1}{2}}+(V_r)^{n+1}_{i-1,j+\frac{1}{2}}}{(\Delta z)^2}\right] \tag{16}$$

Note that $\overline{V_z}$ is calculated using linear interpolation and the next point $(V_r)^{n+1}_{i+1}$ is calculated by extrapolation.

Rearrange Equation (16):

$$\left[1+(\overline{V}_z)^{n+1}_{i,j+\frac{1}{2}}\frac{\Delta t}{\Delta z}+\Delta t\frac{(V_r{}^{n})_{i,j+\frac{1}{2}}}{r_{j+\frac{1}{2}}}+\frac{\mu\Delta t}{\rho r^2_{j+\frac{1}{2}}}-\frac{\mu\Delta t}{\rho}\left(\frac{-2}{\Delta z^2}-\frac{2}{\Delta r^2}\right)\right](V_r)^{n+1}_{i,j+\frac{1}{2}}$$

$$+\left[\Delta t\frac{(V_r)^{n}_{i,j+\frac{1}{2}}}{\Delta r}-\frac{\mu\Delta t}{\rho}\left(\frac{1}{\Delta r^2}+\frac{1}{r_{j+\frac{1}{2}}}\frac{1}{2\Delta r}\right)\right](V_r)^{n+1}_{i,j+\frac{3}{2}}$$

$$+\left[-\Delta t\frac{(V_r)^{n}_{i,j+\frac{1}{2}}}{\Delta r}-\frac{\mu\Delta t}{\rho}\left(\frac{1}{\Delta r^2}-\frac{1}{r_{j+\frac{1}{2}}}\frac{1}{2\Delta r}\right)\right](V_r)^{n+1}_{i,j-\frac{1}{2}}$$

$$=(V_r)^{n}_{i,j+\frac{1}{2}}+\frac{(V_r\,\overline{V}_z)^{n+1}_{i-1,j+\frac{1}{2}}}{\Delta z}\Delta t+\left(\frac{\mu\Delta t}{\rho}\right)\frac{(V_r)^{n+1}_{i+1,j+\frac{1}{2}}+(V_r)^{n+1}_{i-1,j+\frac{1}{2}}}{(\Delta z)^2} \tag{17}$$

Equation (17) can be written in simpler form as follows:

$$b_{j+\frac{1}{2}}(V_r)^{n+1}_{i,j-\frac{1}{2}} + d_{j+\frac{1}{2}}(V_r)^{n+1}_{i,j+\frac{1}{2}} + a_{j+\frac{1}{2}}(V_r)^{n+1}_{i,j+\frac{3}{2}} = c_{j+\frac{1}{2}} \tag{18}$$

where:

$$b_{j+\frac{1}{2}} = \left[1 + \left(\overline{V}_z\right)^{n+1}_{i,j+\frac{1}{2}} \frac{\Delta t}{\Delta z} + \Delta t \frac{\left(V_r{}^n\right)_{i,j+\frac{1}{2}}}{r_{j+\frac{1}{2}}} + \frac{\mu \Delta t}{\rho r^2_{j+\frac{1}{2}}} - \frac{\mu \Delta t}{\rho}\left(\frac{-2}{\Delta z^2} - \frac{2}{\Delta r^2}\right)\right] \tag{19}$$

$$d_{j+\frac{1}{2}} = \left[\Delta t \frac{\left(V_r\right)^n_{i,j+\frac{1}{2}}}{\Delta r} - \frac{\mu \Delta t}{\rho}\left(\frac{1}{\Delta r^2} + \frac{1}{r_{j+\frac{1}{2}}}\frac{1}{2\Delta r}\right)\right] \tag{20}$$

$$a_{j+\frac{1}{2}} = \left[-\Delta t \frac{\left(V_r\right)^n_{i,j+\frac{1}{2}}}{\Delta r} - \frac{\mu \Delta t}{\rho}\left(\frac{1}{\Delta r^2} - \frac{1}{r_{j+\frac{1}{2}}}\frac{1}{2\Delta r}\right)\right] \tag{21}$$

$$c_{j+\frac{1}{2}} = (V_r)^n_{i,j+\frac{1}{2}} + \frac{\left(V_r\,\overline{V}_z\right)^{n+1}_{i-1,j+\frac{1}{2}}}{\Delta z}\Delta t + \left(\frac{\mu \Delta t}{\rho}\right)\frac{(V_r)^{n+1}_{i+1,j+\frac{1}{2}} + (V_r)^{n+1}_{i-1,j+\frac{1}{2}}}{(\Delta z)^2} \tag{22}$$

Equation (18) can be solved by Gauss elimination technique which is programmed in Thomas algorithm.

Pressure gradient correction

The pressure correction technique is a rule used in modeling the flow motion by solving the three dimensional momentum equations in the discretized form to estimate each velocity in each direction and then correcting the pressure gradient in each direction to satisfy the continuity equation. This technique is explained in details in several computational fluid dynamics text books Patankar (1980), Anderson (1995), and Ferziger and Peric (1996).

In this rule it is required to estimate the flow rate at the solved vertical line by numerical integration of the velocity in the axial z-direction and compare it with the inlet one (estimate the error by subtracting the inlet flowrate from the estimated one at the specified line) then increase or decrease the pressure gradient in the cases of negative or positive error respectively. The Laminar code is run at axial no. of nodes n_i = 5002 and radial no. of nodes n_j = 81.

Assume the solving code at line (i+1):

At point (i+1/2, j)

$$dQ = 2*3.14*Radius_{j-1}*dr*(Vz_{i+1/2,j-1}+Vz_{i+1/2,j})/2 \quad (23)$$

$Q = \Sigma dQ$ for the vertical line.

Then calculate the error in Q

$$error = Q - QR \quad (24)$$

where *QR* = Reference flowrate (flowrate at inlet). Now, check if the error in the flowrate is lower than the tolerance or not.

The rule used is called the pressure correction technique and its Flowchart is shown in Figure 3. Note that (X) is the pressure gradient correction term.

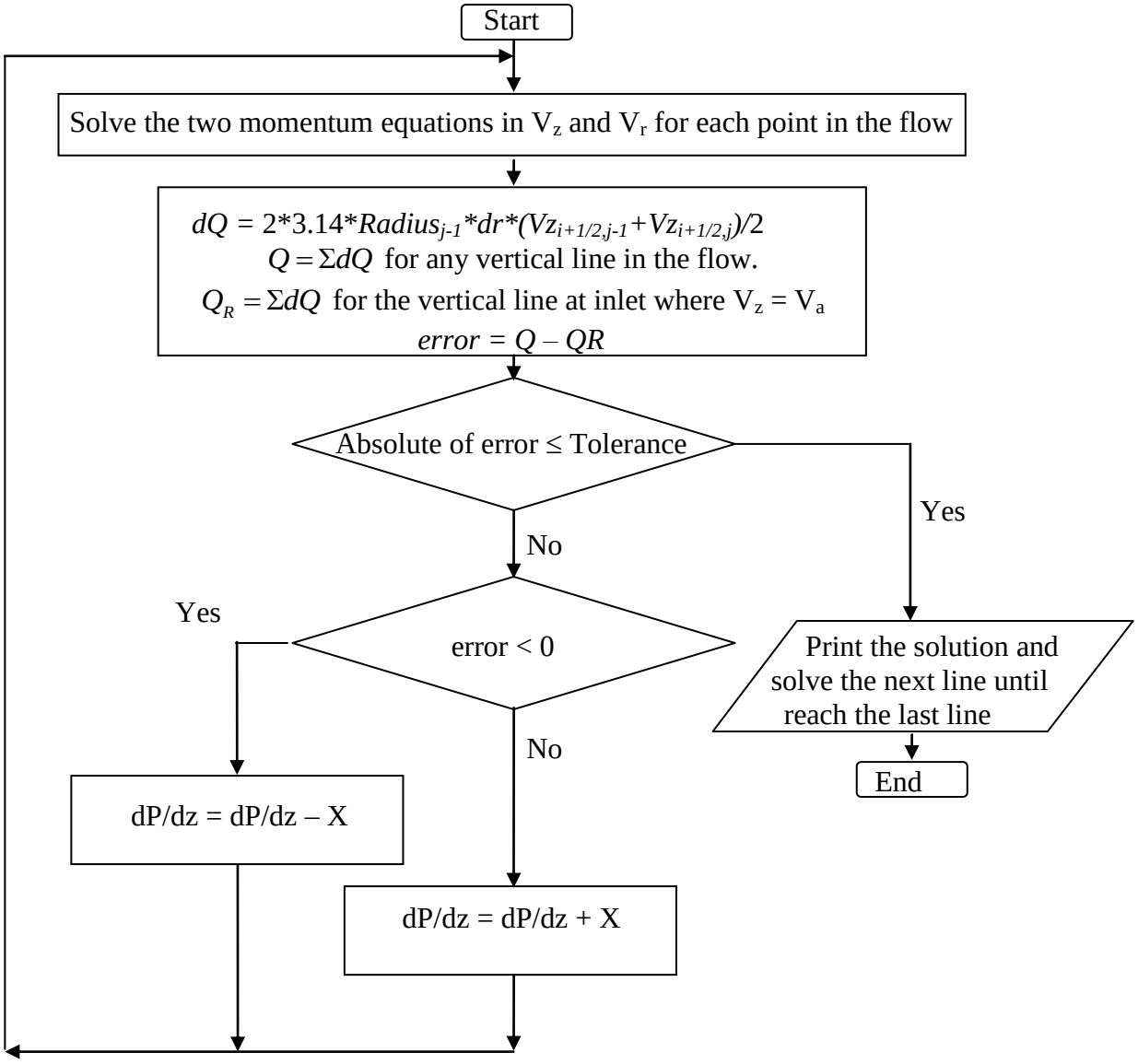

Figure 3 Pressure Correction Flowchart

ANALYTICAL SOLUTION

The fully developed solution for the mentioned case can be obtained analytically which has an exact solution where the flow is Incompressible, Newtonian fluid, laminar and one dimensional. According to Munson et al. (2002), the analytical Momentum equation in Z-direction is:

$$0 = -r\frac{\partial P}{\partial z} + \mu\frac{\partial}{\partial r}[r\left(\frac{\partial V_z}{\partial r}\right)] \tag{25}$$

The analytical Velocity distribution for the flow in an annulus

$$V_z = \frac{1}{4\mu}\frac{dP}{dz}\left[r^2 - r_o^2\right] - \frac{V_c + \frac{1}{4\mu}\frac{dP}{dz}\left[r_o^2 - r_i^2\right]}{\ln\frac{r_o}{r_i}}\ln\frac{r}{r_o} \tag{26}$$

r_o = Pipe radius. r_i = Core radius. r = any radius within annulus.

The drag coefficient relative to both moving core and pipe wall are:

$$C_d = \frac{\tau_w}{\frac{1}{2}\rho V_c^2} \tag{27}$$

Where τ_w =the wall shear stress

$$\tau_w = \mu\left(\frac{r}{2\mu}\frac{dP}{dz} - \frac{V_c + \frac{1}{4\mu}\frac{dP}{dz}[r_o^2 - r_i^2]}{r\ln\frac{r_o}{r_i}}\right) \tag{28}$$

At core wall $r = r_i$
At pipe wall $r = r_o$

RESULTS AND DISCUSSION

The Numerical model is run at the three different diameter ratios kr = 0.8, 0.85, and 0.9 taken from Kroonenberg (1978) at moving core velocity of V_c = 0.1 m/s and at Re_p (where Rep = $[\rho V_a(d_o-d_i)/\mu]$) = 222, 337, 658, 979, and 1621 to predict the fully developed velocity profile for favorable, zero, and adverse pressure gradient, the

developing velocity profiles until reach the fully developed one, the developing length (entrance length), the pressure distribution along the moving core at different Reynolds numbers, and the drag coefficient relative to not only the moving core wall but also the pipe wall at different Reynolds numbers and diameter ratios. Also the results compared with the analytical (exact) solution at the fully developed region.

The dimensionless velocity distribution (V_z/V_c) in annulus with respect to the radius at different Reynolds number is shown in Figure 4. It is obvious that when the Reynolds number is relatively high, the pressure gradient become negative or favorable pressure gradient. As the Reynolds number decreases, the pressure gradient decreases until reaches zero pressure gradient. As the Reynolds number decreases, the pressure gradient becomes adverse until the velocity gradient at the pipe wall becomes zero which leads to zero shear at the pipe wall and that is called flow separation. The pressure distribution is shown in Figure 5 at different Reynolds number. The negative, zero, and the adverse pressure gradient are shown in that figure. In all the previous cases the numerical model results are shown to be in good agreement with the analytical (exact) solution results.

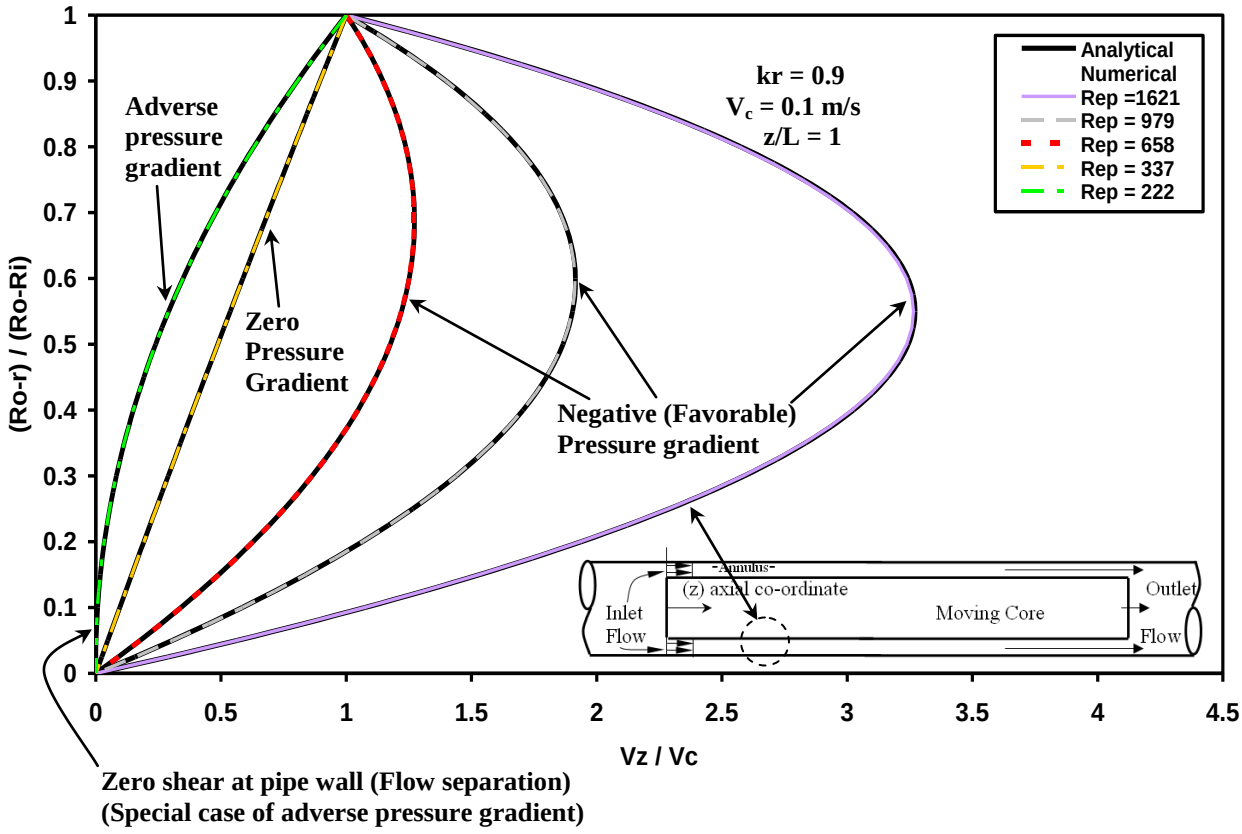

Figure 4 Comparison between numerically and analytically computed fully developed velocity profiles at different Reynolds number

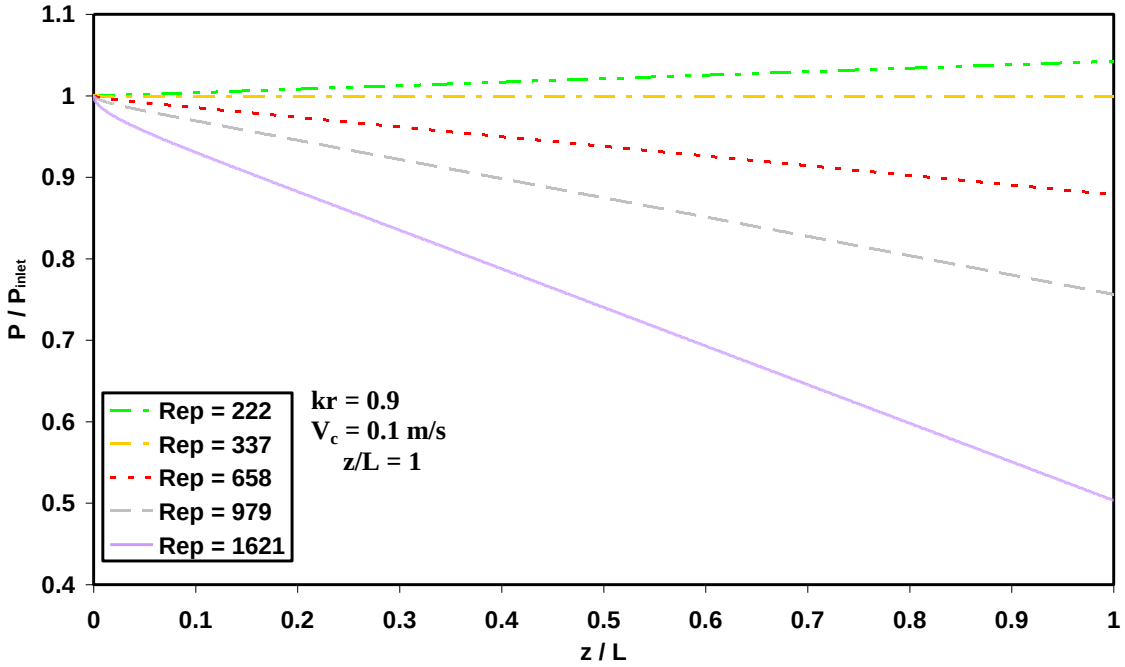

Figure 5 Pressure distribution along the moving core in annulus at different Reynolds number

The dimensionless velocity distribution (V_z/V_c) in annulus along the capsule length is shown in Figure 6. It is clear that the inlet uniform velocity profile is developing and changing until it reaches the fully developed velocity profile which it doesn't change after that. The length in annulus which is taken until the fully developed velocity profile is formed is called the entrance length. In the present case (0.9 diameter ratio kr, Re = 1621, and V_c = 0.1 m/s), the entrance length is equal to 0.16 of the core total length (i.e. $L_{entrance}$ = 0.42 m from L_{core} = 2.64 m). These velocity profiles and the entrance length are calculated numerically by the two dimensional model. Figure 7 shows both the pressure distribution for this case and the entrance pressure drop.

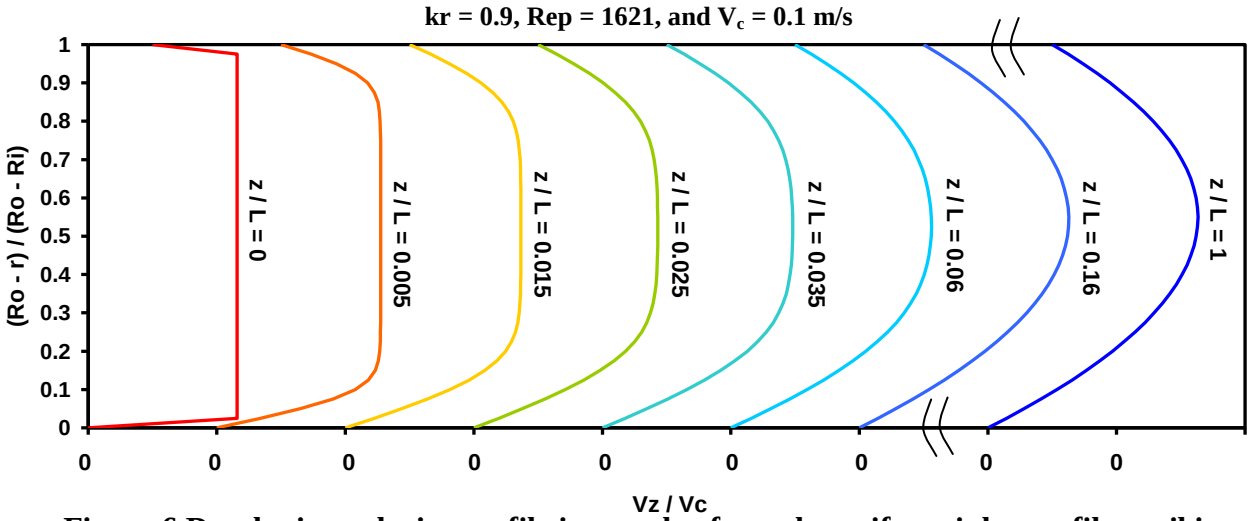

Figure 6 Developing velocity profile in annulus from the uniform inlet profile until it reaches the fully developed one at z / L = 0.16

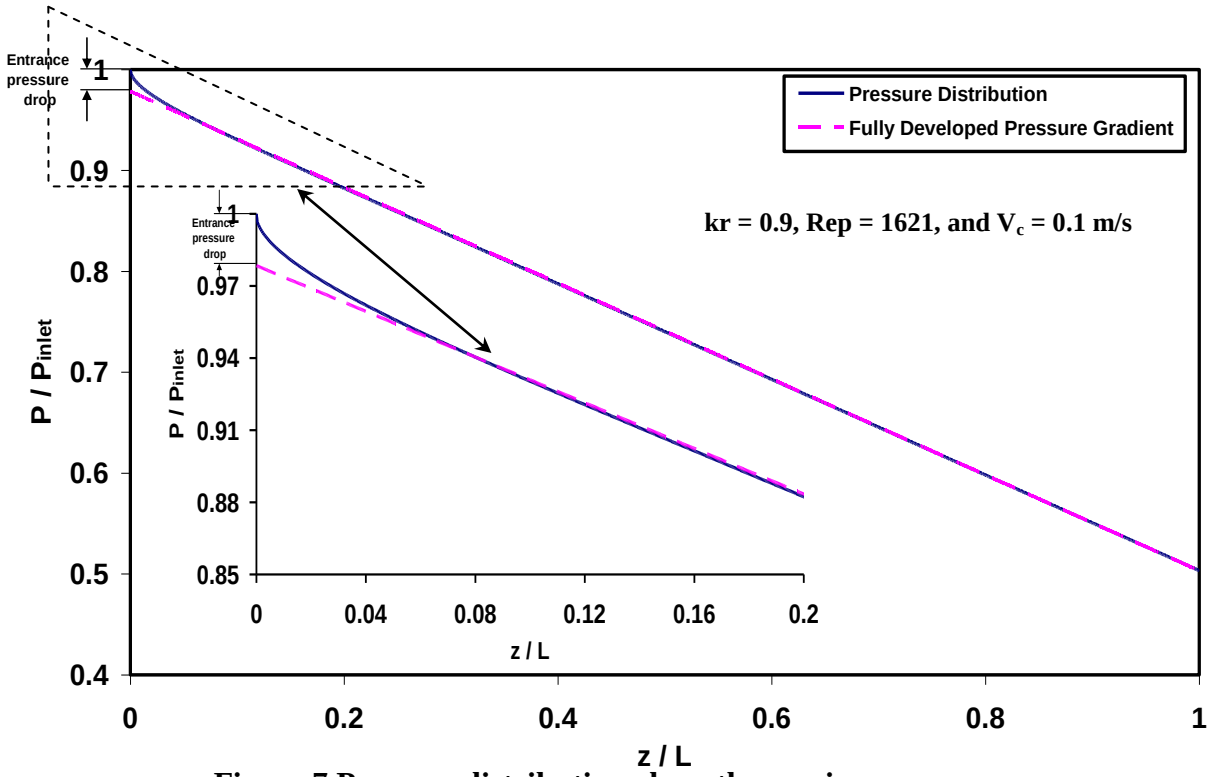

Figure 7 Pressure distribution along the moving core
The entrance pressure drop is also shown (up to z / L = 0.16)

Figure 8 illustrates the distribution of the shear stress within the developing region and the developed one. At the inlet, the shear stress is zero except at the walls where the velocity profile is uniform and the shear stress is obtained from its derivative. The shear stress distribution takes the behavior that tends to reach the fully developed one within the developing region.

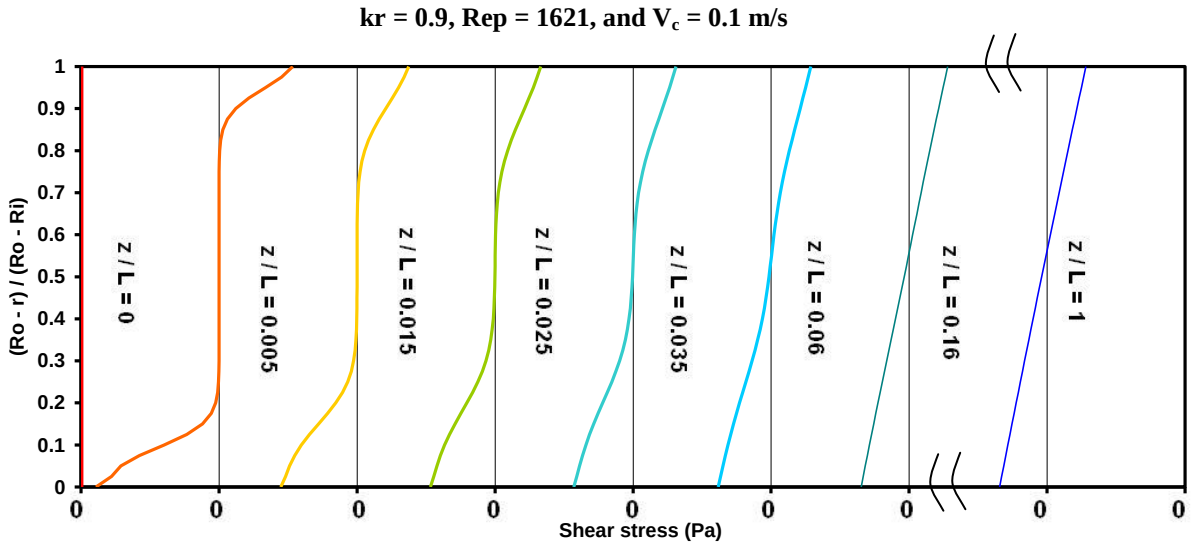

Figure 8 Shear stress distribution within the entrance region and the developed one

Figure 9 illustrates the boundary layer thickness changes within the entrance length. It is obvious that a boundary layer in which viscous effects are important is produced along both the moving core and the pipe wall such that the initial velocity profile changes with distance along the core, z-direction, until the fluid reaches the end of the entrance length beyond which the velocity profile does not vary with z. The boundary layer has grown in thickness to completely fill the annulus. Viscous effects are of considerable importance within the boundary layer. For fluid outside the boundary layer [within the inviscid core surrounding the centerline of the annulus], viscous effects are negligible.

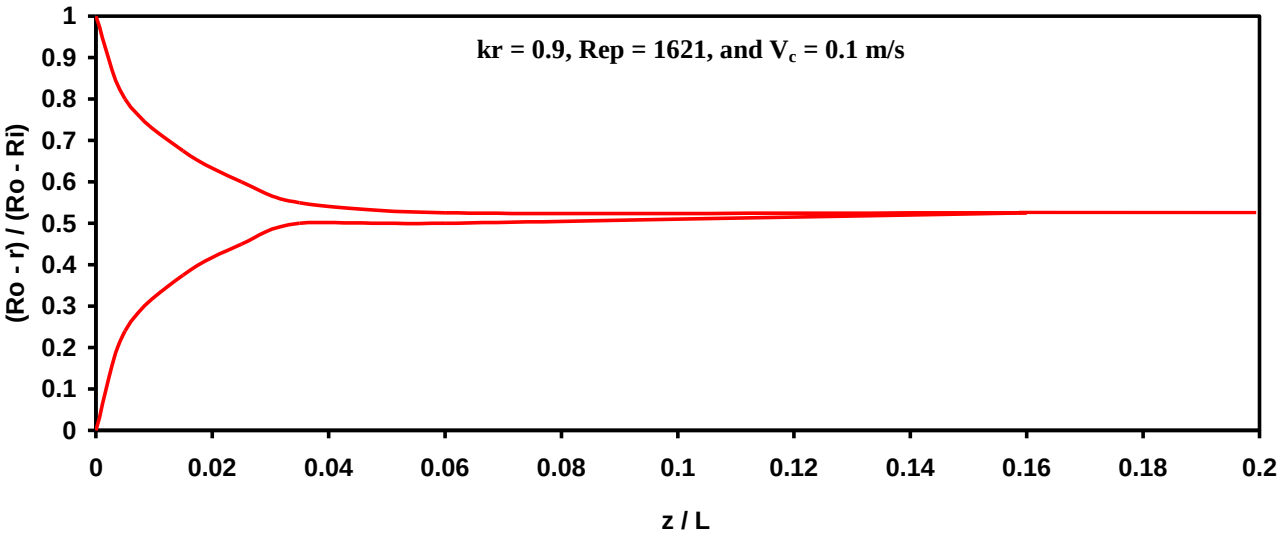

Figure 9 Boundary layer thickness changes within the entrance length

Figure 10 illustrates the drag coefficient relative to the moving core wall distribution within the developing region. The drag coefficient relative to the moving core wall is maximum at the inlet where the wall shear stress is maximum also. Then the drag coefficient reduces within the entrance region until it reaches the fully developed one. The drag coefficient relative to moving core wall and to pipe wall are compared with the analytical (exact) solution at different Reynolds number and different diameter ratios as shown in Figures 11 (a, b).

From Figure 11(a, b), it is clear that as the annulus becomes narrower (i.e. the diameter ratio is increased), the drag coefficient increases. This is due to the increase in the pressure drop. Furthermore, as the Reynolds number increases, the drag coefficient increases for the same reason. These two figures show that the numerical results are in a good agreement with the analytical (exact) one. Note that in Figure 11-a, the positive drag means that the shear stress exerts in the moving core is in the same direction of core velocity and vice versa the negative drag.

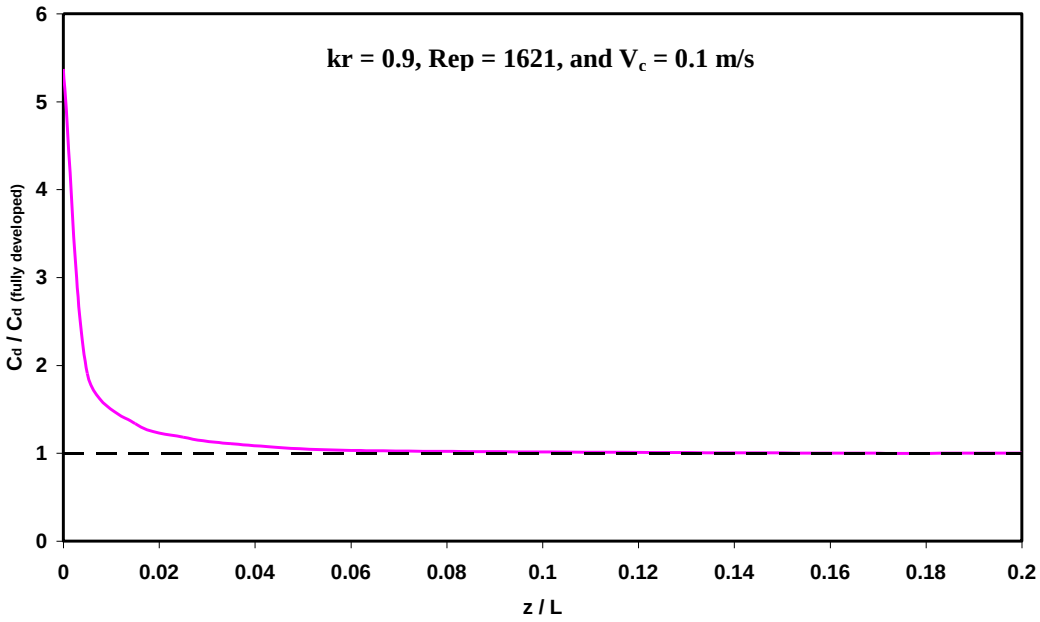

Figure 10 Core drag coefficient within the developing region

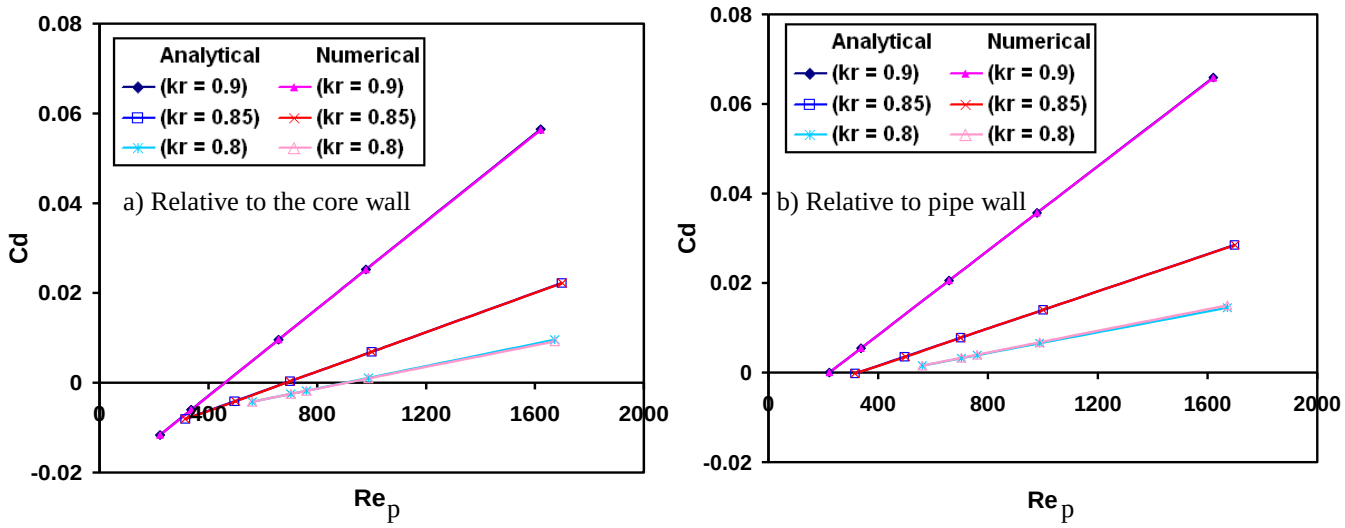

Figure 11 Drag versus Reynolds number for different diameter ratios (kr)

Figure 12 illustrates the numerically computed drag coefficient versus the analytically computed one. It is shown that the numerically computed drag coefficient is in good agreement with the analytically computed one at different Reynolds numbers and at different diameter ratios. These results ensure that the numerical model is valid at a wide range of Reynolds number (Laminar only) and in the recommended range of the diameter ratios (kr) practical applications of Hydraulic Capsule Pipeline (HCP).

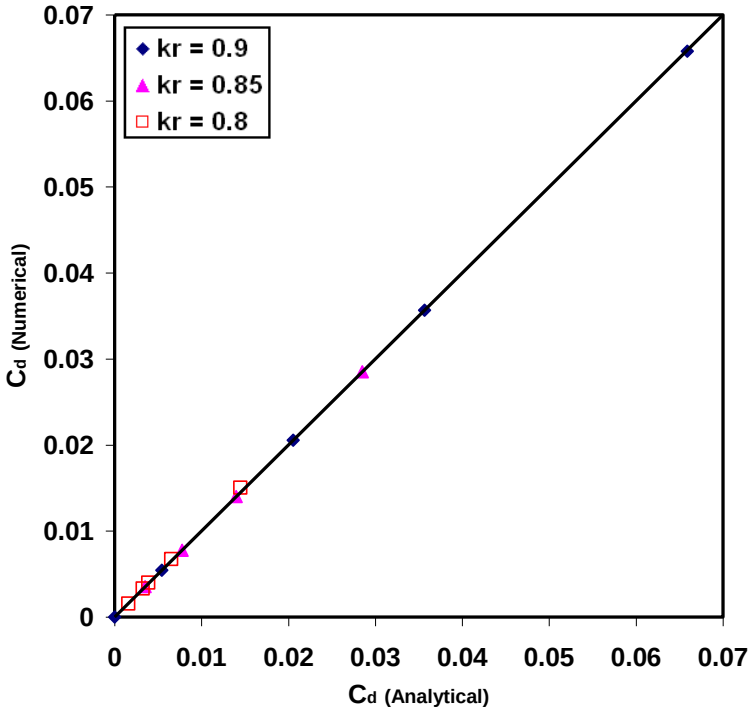

Figure 12 The numerically computed drag coefficient vs. the analytically computed one

CONCLUSIONS

The present study of the laminar modeling provides a two-dimensional, axi-symmetric, steady model to predict the flow properties in concentric annulus. The model is used to predict the velocity profile in annulus and show its variation with Reynolds number for favorable, zero and adverse pressure gradient. The flow separation is obtained in the case of adverse pressure gradient. The pressure and the drag coefficient distributions along the moving core length are obtained also at different Reynolds number. The developing in both velocity profile and the shear stress distribution until reaching the fully developed region is predicted. The boundary layer thickness in developing region is predicted along the moving core length. The model is verified by checking its results with the analytical results and it gives a good agreement along a wide range of Reynolds numbers and the recommended diameter ratios. All of that ensure the validity of the used equations, finite difference scheme, and the solving technique. This model can be used as the first step towards establishing a turbulent model to solve the practical cases of capsule flow in the Hydraulic Capsule Pipeline (HCP).

REFERENCES

Anderson, J. D. (1995). "Computational Fluid Dynamics". McGraw-Hill, Inc., USA.

Ferziger, J. H., and Peric, M. (1996). "Computational Methods for Fluid Dynamics", Springer-Verlag Berlin Heidelberg New York.

Fujiwara, Y., Tomita, Y., Satou, H., and Funatsu, K. (1994). "Characteristic of Hydraulic Capsule Transport." JSME International Journal, Vol. 37, pp. 89 - 95.

Garg, V. K. (1977). "Capsule Pipelining-An Improved Theoretical Analysis." Journal of Fluids Engineering, Transactions of ASME, pp. 763-771.

Garner, R. G., and Raithby G. D. (1978). "Laminar Flow between a Circular Tube and a Cylindrical Eccentric Capsule." Canadian Journal of Chemical Engineering, Vol. 56, pp. 176-180.

Govier, G. W., and Aziz, K. (1972). "The Flow of Capsules in Pipes." The flow complex mixtures in pipes. Van Nostrand-Reinhold, New York, N.Y.

Liu, H. (2003). "Pipeline Engineering", Lewis Publishers, CRC Press Company, USA.

Munson, B. R., Young, D. F., and Okiishi, T. H. (2002). "Fundamentals of Fluid Mechanics". John Wiley & Sons, Inc., Hoboken, USA.

Ogawa, K., Ito, S., and Kuroda, C. (1980). "Laminar-Turbulent Velocity Profile Transition for Flows in Concentric Annuli, Parallel Plates and Pipes." Journal of Chemical Engineering of Japan, Vol. 13, pp. 183-188.

Patankar, S. V., (1980), "NUMERICAL HEAT TRANSFER AND FLUID FLOW", Hemisphere Publishing Corporation, McGraw-Hill Book Company., USA.

Samaha, M. (2007). "Numerical Simulation of the Flow through Hydraulic Capsule Pipeline." M.Sc. Thesis, Faculty of Engineering, Alexandria University, Alexandria 21544, Egypt.

Tachibana, M. (1983). "Balance and startup of Cylindrical Capsule in Rising Flow of Inclined Pipeline." Bulletin of the JSME, Vol. 26, pp. 1735-1743.

The ASCE Task Committee on Freight Pipelines of the Pipeline Division. (1998). "Freight Pipelines: Current Status and Anticipated Future Use," Journal of Transportation Engineering, Transactions of ASCE, Vol. 124, pp. 300-310.

Tomita, Y., and Fujiwara, Y. (1992), "Capsule Velocity in Pipelines." JSME International Journal, Vol. 35, pp. 513-518.

Tomita, Y., ABE, K., and Jotaki, T. (1981), "Analysis of Capsule Pipeline System by the Method of Characteristics." Bulletin of the JSME, Vol. 24, pp. 1579-1585.

Tsuji, Y., Morikawa Y., Chono, S., and Hasegawa, T. (1984), "Wake of capsule and the effect of interaction between two capsules on the drag." Bulletin of the JSME, Vol. 27, pp. 468-474.

van den Kroonenberg, H. H. (1978), "A Mathematical Model for Concentric Horizontal Capsule Transport." The Canadian Journal of Chemical Engineering, Vol. 56, pp. 538-543.